TASK QUARTERLY 13 No 3, 187–197

STABILITY OF FINITE-SIZE ARGON THIN FILM COATING SINGLE WALL CARBON NANOTUBE

MARCIN KOŚMIDER[1], ZBIGNIEW DENDZIK[2], SEBASTIAN ŻUREK[1] AND KRZYSZTOF GÓRNY[2]

[1]*Institute of Physics, University of Zielona Gora, Prof. Szafrana 4a, 65-516 Zielona Gora, Poland*
M.Kosmider@proton.if.uz.zgora.pl

[2]*Institute of Physics, University of Silesia, Uniwersytecka 4, 40-007 Katowice, Poland*

(Received 1 September 2008; revised manuscript received 15 February 2009)

Abstract: The structure and the dynamics of the argon thin film coating (15,4) and (12,12) carbon nanotubes have been studied in a series of molecular dynamic simulations. In the studied temperature regime, the argon atoms in the thin film were well localized. Structural changes and diffusion process inside the argon layers were not been observed. The influence of the chirality and the radius of the nanotube to the cluster properties is also reported.

Keywords: nanotube, molecular dynamics, cluster, thin film

1. Introduction

In the recent decades, considerable interest, both experimental and theoretical, has been devoted to study the free atomic and molecular clusters. Due to their specific – finite size properties the systems are significantly different from the bulk materials [1–4]. From the technological point of view, development and production of a new materials with tailored properties require to deposit clusters on a surface. Thus, it is crucial to understand the process of deposition as well as the structural and dynamical properties of nano-structures created by cluster deposition on surface. Low energy deposition can prevent cluster fragmentation and surface damages but, as many experimental and molecular dynamics studies have shown, "soft landed" clusters can migrate on surface with high diffusion coefficient comparable to that of adatoms [5–7]. The key to understand this phenomenon is the mismatch between cluster and surface [8, 9]. If no fast diffusion is observed, the deposition process can lead to epitaxial growth of thin film, which morphology and properties strongly depending on the energy of cluster deposition [10–12]. The unique honeycomb cylindrical surface of carbon nanotubes and nanotube boundles gives great opportunity not

only for testing properties of nanomaterials like nanowires, gas sensors or gas storage containers [13–15], but also as a templates for formation 1D, 2D and 3D adsorbate phases [16–18]. Zhang and Dai showed that various metals deposited on a single-wall carbon nanotube by a evaporation process forms separated clusters on the nanotube surface due to weak interactions between the metals and nanotubes [19]. When the nanotube was coated by a buffer layer of titanium atoms, growth of a continue metal nanowires on nanotube surface was observed. Based on the first principle calculations, Bagci *et al.* found that formation of aluminium nanoring and nanowire surrounding carbon nanotubes was possible and depends on the adsorption sites [20]. The molecular dynamics simulations of exohedral complexes of argon cluster and rigid (10,10) carbon nanotube showed that argon clusters are stable up to 40 K and up to this temperature the diffusion in cluster was not observed [21]. The lack of liquid phase in deposited icosahedral 13-atom cluster on flat surface was also observed in molecular dynamics simulation performed by Sun and Gong [8].

In this paper, we report molecular dynamics simulation studies of structural and dynamical properties of finite-size argon thin film coating (15,4) and (12,12) single walled carbon nanotubes. The fact that (15,4) nanotube differs in structure but has almost identical diameter as examined earlier [21] (10,10) nanotube provide a direct opportunity to test the influence of nanotube chirality to the cluster properties. On the other hand, the effect of the nanotube diameter to the cluster properties can be examined with (12,12) nanotube which structure is the same as the (10,10) nanotube, but its diameter is different. Due to the finite size of the thin film and its specific properties resulting from the free edges we prefer to name the investigated thin film cluster or cluster-like system.

2. Simulation details

In order to determine the properties of exohedral complexes composed of argon cluster coating carbon nanotube, the molecular dynamics simulations of monolayer and bilayer argon cluster-like thin film coating (15,4) and (12,12) carbon nanotubes have been performed. In the case of (15,4) nanotube 140 and 280 argon atoms were used to build the monolayer and bilayer thin film, respectively. With (12,12) nanotube used as a template, the monolayer cluster was composed of 171 and 319 argon atoms were used to build the bilayer cluster. The initial configuration of clusters that corresponds to the minimum energy structure has been obtained by Metropolis Monte Carlo scheme, where the configuration with ideal compact structure (with no holes) and without adatoms in next layer has been only used. Next, the system was heated up with the velocity scaling method. When the desired temperature was achieved, in the second part of the equilibration the thermostat has been turned off. After the equilibration stage, the main simulation was started. The final configuration generated at each temperature was heated up to be used as a new starting configuration for the next specific temperature and the same equilibration procedure was performed.

The interactions between the argon atoms in cluster were modelled with the HFD-B potential developed by Aziz [22]:

$$V(r_{ij}) = \epsilon_a V^*(x_{ij}), \tag{1}$$

where

$$V^*(x_{ij}) = A^* \exp(-\alpha^* x_{ij} + \beta^* x_{ij}^2) - F(x_{ij}) \sum_{j=0}^{2} \frac{c_{2j+6}}{x_{ij}^{2j+6}}, \tag{2}$$

$$F(x_{ij}) = \begin{cases} \exp[-(D/x_{ij}-1)^2] & x_{ij} < 0 \\ 1 & x_{ij} \geq 0 \end{cases}, \tag{3}$$

$$x_{ij} = \frac{r_{ij}}{r_m}. \tag{4}$$

The values of parameters A^*, α^*, β^*, c_6, c_8, c_{10}, D, r_m, ϵ_a are collected in Table 1.

Table 1. Parameters of the HFD-B Ar-Ar potential

Parameters	Value
A^*	8739.3927
α^*	9.03228328
β^*	−2.37132823
c_6	1.0948575
c_8	0.5917572
c_{10}	0.3450815
D	1.4
r	0.3759 nm
ϵ_a	1.1190334664 kJ/mol

The adsorption potential between the nanotube and the cluster atoms was modelled as a sum of the Lennard-Jones (LJ) two-body interaction between the C atoms in nanotube and the argon atoms in cluster:

$$V_{\mathrm{LJ}}(r_{ij}) = 4\epsilon_{\mathrm{Ar-C}} \left(\frac{\sigma_{\mathrm{Ar-C}}^{12}}{r_{ij}^{12}} - \frac{\sigma_{\mathrm{Ar-C}}^{6}}{r_{ij}^{6}} \right) \tag{5}$$

with the parameters: $\epsilon_{\mathrm{Ar-C}} = 57.96\,\mathrm{K}$ and $\sigma_{\mathrm{Ar-C}} = 0.34\,\mathrm{nm}$ [23].

For the inter-molecular interactions between the nanotube carbon atoms the valence force field include Morse potential, harmonic angle potential and torsion potential for bonded atom and LJ potential for nonbonded carbon atoms were used [24, 25]:

$$V = V_{\mathrm{bond}} + V_{\mathrm{LJ}}, \tag{6}$$

$$\begin{aligned} V_{\mathrm{bond}}(r_{ij}, \Theta_{ijk}, \varphi_{ijkl}) = & K_r (e^{-\gamma(r_{ij}-r_c)} - 1)^2 + \tfrac{1}{2} K_\Theta (\cos\Theta_{ijk} - \cos\Theta_c)^2 + \\ & + \tfrac{1}{2} K_\varphi (1 - \cos 2\varphi_{ijkl})^2, \end{aligned} \tag{7}$$

where r_{ij} is a distance between the given pair of bonded atoms, Θ_{ijk} is the bending angle between the given three atoms and φ_{ijkl} is the torsional angle between the given four atoms. The values of potential parameters for nanotube are given in Table 2.

Table 2. Parameter of the carbon interaction potentials

K_r [kJ/mol]	K_Θ [kJ/mol]	K_φ [kJ/mol]	γ [nm^{-1}]	r_c [nm]	Θ_c [°]	σ [nm]	ϵ [kJ/mol]
478.9	562.2	25.12	0.21867	0.1418	120	0.3851	0.4396

To characterize the cluster structure with the temperature and the nanotube chirality changes the radial distribution function of cluster atoms:

$$g(r) = \sum_{i=1}^{N} \frac{n_i(r, r+\Delta r)}{4\pi r^2 \Delta r} \tag{8}$$

was calculated, where $n_i(r, r+\Delta r)$ is the number of the atoms in spherical shell with thickness Δr and given radius r from i-th atom. This function gives information about the population of atoms at distance between r and $r+\Delta r$ relative to any particle in the cluster and informs about the structure of investigated cluster.

The mobility of the atoms in the cluster was analysed in terms of relative root-mean-square (rms) bond length fluctuations:

$$\delta = \frac{2}{N(N-1)} \sum_{i<j} \frac{\sqrt{\langle r_{ij}^2 \rangle - \langle r_{ij} \rangle^2}}{\langle r_{ij} \rangle}, \tag{9}$$

where r_{ij} is the distance between atoms i and j, and the sum is over all atoms. That quantity describes also the stiffness of cluster and enables the determination of the cluster melting temperature.

The behaviour of the dynamical properties of the cluster was monitored by a spectral density defined as the cosine Fourier transform of the normalized velocity autocorrelation function:

$$I(\nu) = \int_0^\infty C_v(t) \cos(2\pi\nu t) dt, \tag{10}$$

where

$$C_v(t) = \frac{\langle V(0)V(t) \rangle}{\langle V(0)^2 \rangle} \tag{11}$$

is the normalized velocity autocorrelation function.

This spectral density corresponds to the phonon density of states, *i.e.* the number of vibrational modes in a given frequency interval, and gives informations of the transitions from solid-like to liquid-like phase.

3. Results and discussion

3.1. Clusters coating (15,4) *nanotube*

The monolayer cluster composed of 140 argon atoms and 280 argon atoms bilayer cluster forming cylindrical, concentric thin film coating carbon nanotube was studied in the temperature regime ranged from $T = 14\,\mathrm{K}$ to $T = 36\,\mathrm{K}$. Above the 36 K the argon atoms creating the edges of the cluster started to evaporate. The evaporated atoms remained adsorbed on the nanotube surface but the cluster lost its integrity and these cases were excluded from the further analyses.

The snapshot of the equilibrium structures of the simulated systems are shown in Figure 1. The cluster forms coaxial cylindrical shells commensurate with the nanotube substrate. Shells are composed of spiral rows of argon atoms that are not parallel to the nanotube axis. The arrangement of the argon atoms reflects the nanotube chirality, what can be clearly observed in the edges of the cluster where the argon nanorings are not perpendicular to the nanotube axis. No structural changes

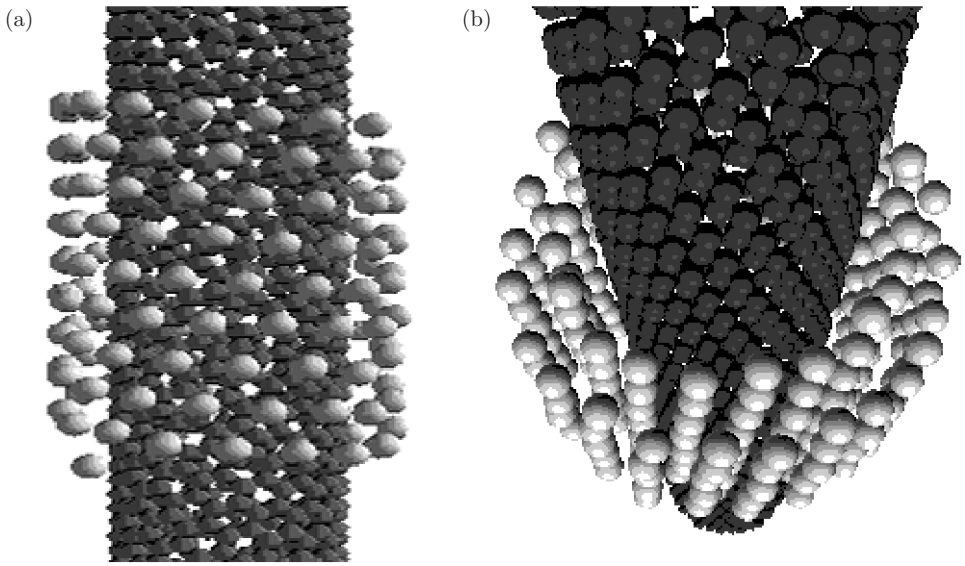

Figure 1. A snapshot of (a) monolayer; (b) bilayer argon cluster surrounding the (15,4) nanotube

were observed when the temperature was increased. The spatial structure of the argon shells have been studied in terms of the radial distribution function. Figure 2 shows the $g(r)$ function for monolayer (Figure 2a) and bilayer (Figure 2b) cluster in the lowest and the highest of the considered temperatures. The temperature does not significantly change the position of the characteristic peaks on the $g(r)$ function plot, which suggest that there are no structural changes in the cluster. The cluster remains solid-like with highly localized argon atoms positions with except to the edges of the cluster where some migrations of atoms between rows are possible at higher temperatures. This results are also visible on the Figure 3a which visualises the rms bond length fluctuation as a function of temperature. The rms bond length fluctuation δ is a standard quantity measure in cluster simulations. According to the Lindemann's criterion the system is liquid when $\delta > 0.1$. In the whole studied temperature regime rms bond length fluctuation is less than 0.1.

The dynamics of the system has been studied in terms of power spectrum $I(\nu)$ of the velocity autocorrelation function. This very informative quantity gives possibility to discern quasi periodic motion in solid-like phase from the chaotic motion in liquid-like phase. According to the Green-Kubo relation, $I(\nu = 0)$ is proportional to the diffusion coefficient. Figure 4 shows the power spectrum of the velocity autocorrelation function of the monolayer (Figure 4a) and the bilayer (Figure 4b) cluster-like thin film coating carbon nanotube at the temperatures $T = 14\,\mathrm{K}$ (solid line) and $T = 36\,\mathrm{K}$ (dotted line). The well localized sharp peaks and absence of translational diffusion ($I(0) = 0$) are characteristic features of the solid-like phase. In the case of monolayer cluster the well characterised frequency at $\nu \simeq 40\,\mathrm{cm}^{-1}$ is observed only in radial component of the velocity power spectrum and it can be assigned to oscillatory radial movements of the argon atoms to the nanotube surface. The tangential and axial components of the velocity autocorrelation power spectrum is composed of the broad distribution and no sharp frequencies are observed. The

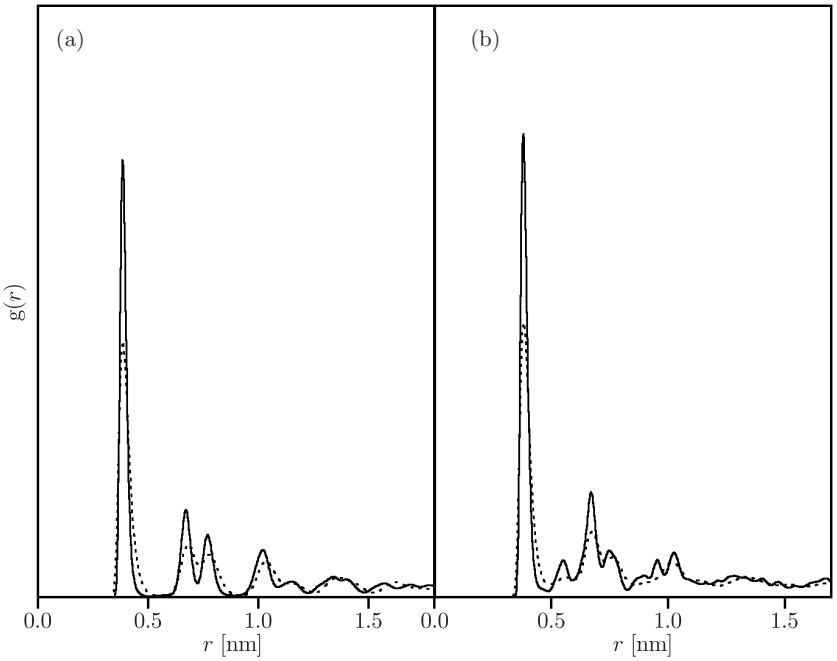

Figure 2. The radial distribution function $g(r)$ of the (a) monolayer argon cluster surrounding (15,4) nanotube at temperature $T = 14\,\mathrm{K}$ (solid line) and $T = 36\,\mathrm{K}$ (dotted line); (b) bilayer argon cluster surrounding (15,4) nanotube at $T = 14\,\mathrm{K}$ (solid line) and $T = 36\,\mathrm{K}$ (dotted line)

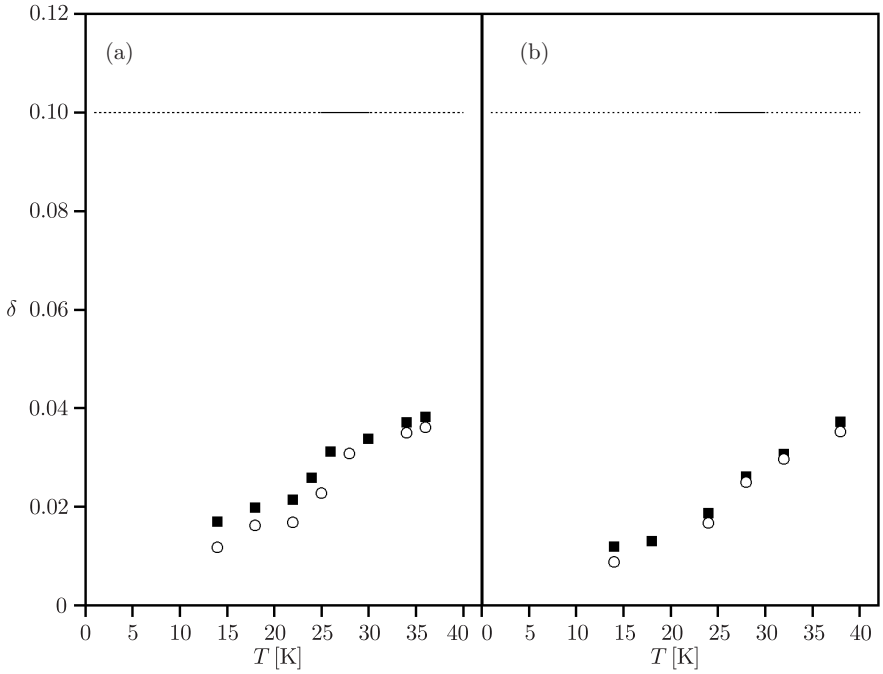

Figure 3. Rms bond length fluctuation as function of temperature for (a) monolayer cluster (black square) and bilayer cluster (open circle) surrounding (15,4) nanotube; (b) monolayer cluster (black square) and bilayer cluster (open circle) surrounding (12,12) nanotube

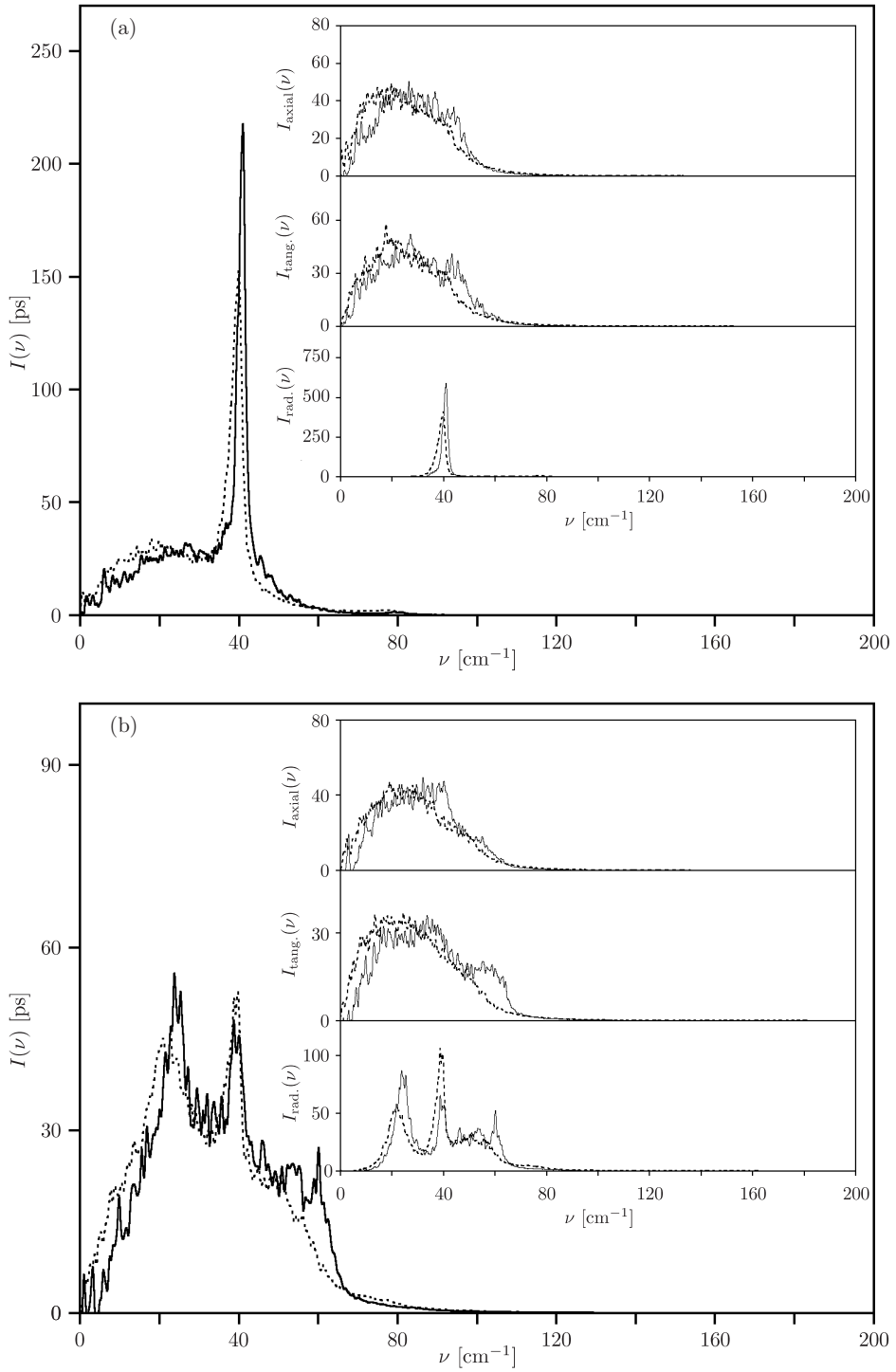

Figure 4. Spectral density $I(\nu)$ of the (a) monolayer argon cluster surrounding (15,4) nanotube at temperature $T = 14\,\mathrm{K}$ (solid line) and $T = 36\,\mathrm{K}$ (dotted line); (b) bilayer cluster surrounding (15,4) nanotube at temperature $T = 14\,\mathrm{K}$ (solid line) and $T = 36\,\mathrm{K}$ (dotted line). The insets shows the radial $I_{\mathrm{rad}}(\nu)$, tangential $I_{\mathrm{tang.}}(\nu)$ and axial $I_{\mathrm{axial}}(\nu)$

characteristic, radial frequency at $\nu \simeq 40\,\mathrm{cm}^{-1}$ is also distinctly visible in the bilayer cluster's power spectrum. In this case the two characteristic frequencies are also visible in radial component of the power spectrum at frequencies $\nu \simeq 23\,\mathrm{cm}^{-1}$ and $\nu \simeq 60\,\mathrm{cm}^{-1}$ – these are not observed in monolayer cluster. The appearance of the frequencies is related to the interactions between atoms in inner and outer shell. The shape of the power spectrum does not depend on the temperature. The characteristic solid-like – liquid-like transition shift to lower frequencies, appearance of translational diffusion ($I(\nu) \neq 0$) and broadening of the power spectrum in studied systems were not observed.

3.2. Clusters coating (12,12) *nanotube*

The snapshot of equilibrium structure of monolayer cluster and bilayer cluster surrounding (12,12) carbon nanotube is presented in Figure 5. In this case the argon cluster consist of 171 (monolayer cluster) and 319 (bilayer cluster) atoms. The arrangement of the argon atoms in the shells reflects the nanotube structure. In opposite to the exohedral complex with (15,4) nanotube, the rows of atoms are parallel to the nanotube axis. This structure was stable up to $T = 38\,\mathrm{K}$ and above this temperature the edges atoms from cluster start to evaporate. The radial distribution function is plotted in Figure 6 for $T = 14\,\mathrm{K}$ and $T = 38\,\mathrm{K}$. As in previous studied system with (15,4) nanotube the structural changes with increasing temperature is not observed. The chirality and the radius of the nanotube does not significantly change the interatomic distance between the argon atoms in cluster what is visible in Figure 6 presenting radial distribution function for monolayer cluster at $T = 14\,\mathrm{K}$ coating (15,4) and (12,12) nanotube. To test the existence of the solid-like – liquid-like phase transition in the system, the rms bond length fluctuation was calculated for the various temperatures from the studied temperature regime. The result is presented in Figure 3b.

The characteristic frequencies of motion of the argon atoms in the cluster surrounding (12,12) nanotube are shown in Figure 7. Because of the fact, that in whole range of studied temperature no structural changes were observed, only the low temperature spectral densities are presents. As in previous cases, the characteristic frequencies are associated with oscillatory movement of argon atoms radially to the nanotube. The characteristic sharp peaks are located at $\nu \simeq 23\,\mathrm{cm}^{-1}$, $\nu \simeq 40\,\mathrm{cm}^{-1}$ and $\nu \simeq 58\,\mathrm{cm}^{-1}$.

4. Conclusions

The structural and dynamical properties of exohedral complexes composed of cluster forming thin film coating nanotubes with chiralit (15,4) and (12,12) have been studied using the molecular dynamics simulation. Opposite to our former simulations, in this cases the nanotubes were treated as flexible. We showed, that the argon clusters coating nanotube are stable up to $T = 38\,\mathrm{K}$ in the case of armchair nanotube and up to $T = 36\,\mathrm{K}$ in the case of the chiral nanotube and in whole studied temperature regime where cluster retains its integrity no liquid phase and no structural changes has been observed, with the exception to the edges of the cluster, where some atom migration between argon rows are possible. Well localized characteristic frequencies were found at $\nu \simeq 40\,\mathrm{cm}^{-1}$ for monolayer and bilayer cluster. In the case of bilayer

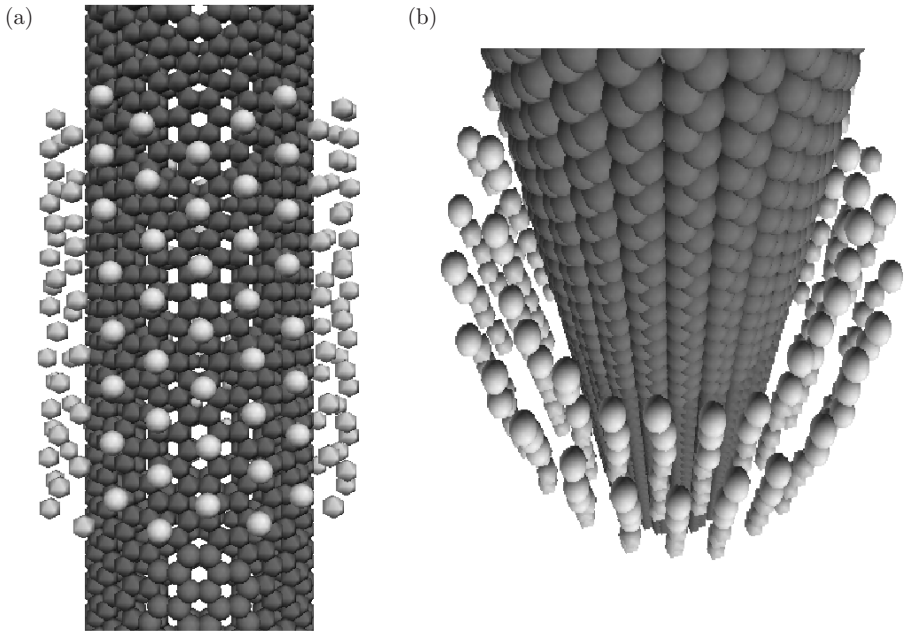

Figure 5. A snapshot of (a) monolayer; (b) bilayer argon cluster surrounding the (12,12) nanotube

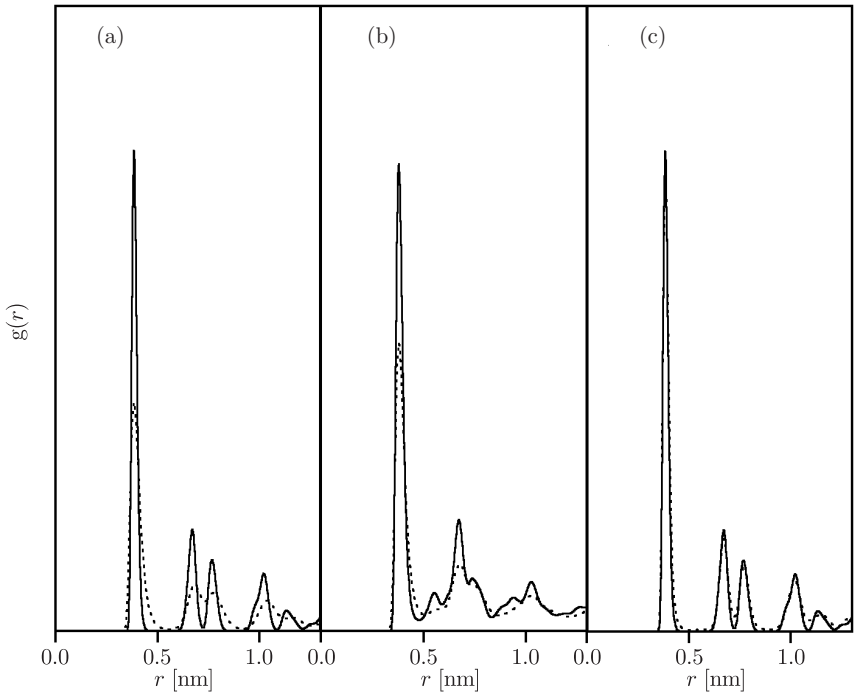

Figure 6. The radial distribution function $g(r)$ of the (a) monolayer argon cluster surrounding (12,12) nanotube at temperature $T = 14\,\mathrm{K}$ (solid line) and $T = 36\,\mathrm{K}$ (dotted line); (b) bilayer argon cluster surrounding (12,12) nanotube at $T = 14\,\mathrm{K}$ (solid line) and $T = 36\,\mathrm{K}$ (dotted line); the figure (c) shows the radial distribution function at $T = 14\,\mathrm{K}$ of monolayer cluster surrounding (12,12) nanotube (solid line) and (15,4) nanotube (dotted line)

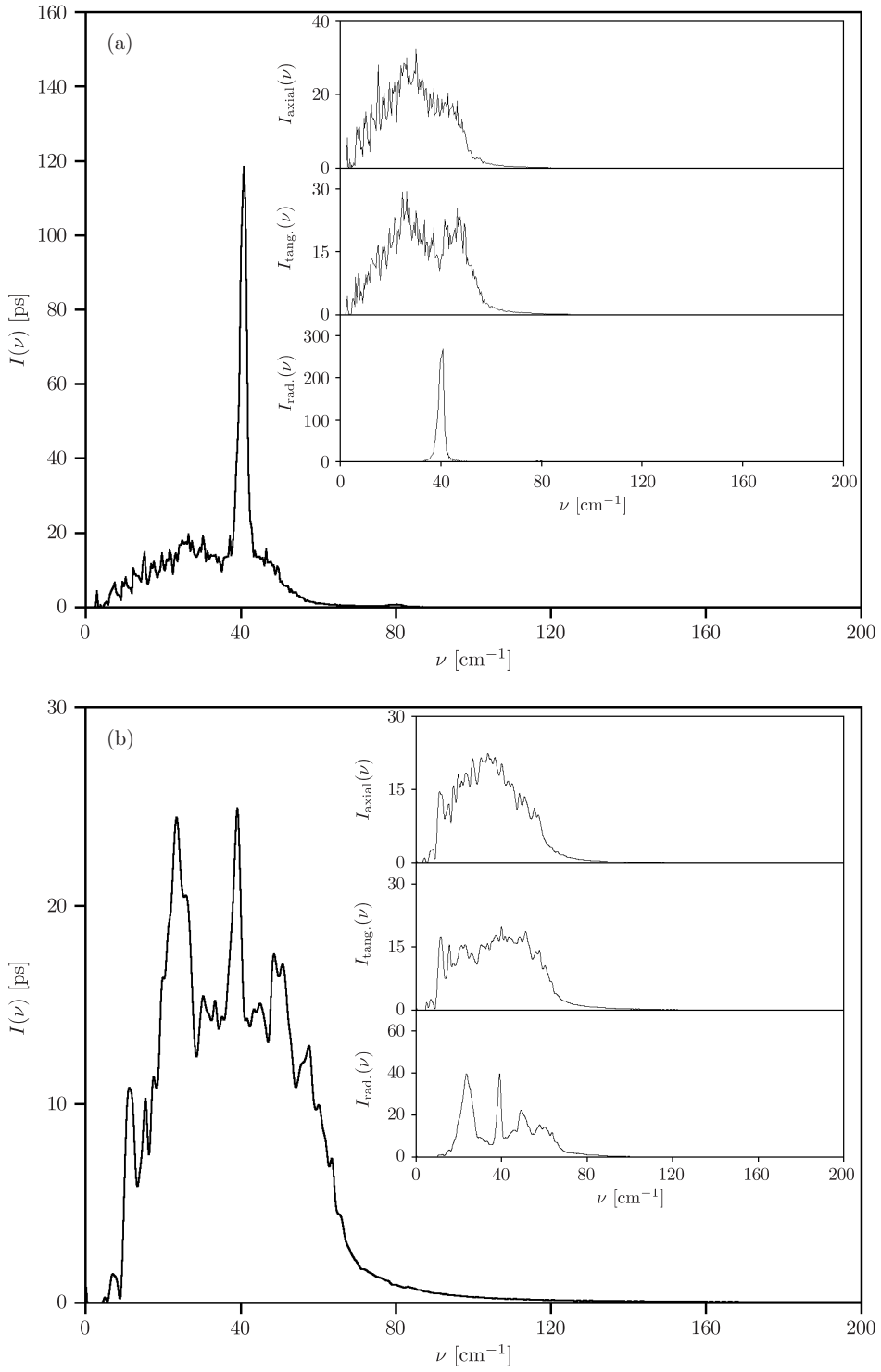

Figure 7. Spectral density $I(\nu)$ of the (a) monolayer argon cluster surrounding (12,12) nanotube at temperature $T = 14\,\mathrm{K}$; (b) bilayer cluster surrounding (12,12) nanotube at temperature $T = 14\,\mathrm{K}$. The insets shows the radial $I_{\mathrm{rad}}(\nu)$, tangential $I_{\mathrm{tang.}}(\nu)$ and axial $I_{\mathrm{axial}}(\nu)$

cluster, besides this frequency, the two new frequencies resulting from interaction between inner and outer cluster shell appear at $\nu \simeq 23\,\mathrm{cm}^{-1}$ and at $\nu \simeq 58\,\mathrm{cm}^{-1}$. The radius of $(15,4)$ is almost identical to the radius of $(10,10)$ nanotube ($r = 0.679\,\mathrm{nm}$ and $r = 0.678\,\mathrm{nm}$ respectively) but the chirality is different. The $(12,12)$ nanotube has the radius $r = 0.813\,\mathrm{nm}$ and the chirality the same as $(10,10)$ nanotube. The comparison of the result for these three cases clearly shows that neither radius nor chirality does not significantly change the structural and dynamical properties of the argon cluster surrounding the carbon nanotube.

References

[1] Martin T P 1996 *Phys. Rep.* **273** 199
[2] de Heer W A 1993 *Rev. Mod. Phys.* **65** 611
[3] Brack W A 1993 *Rev. Mod. Phys.* **65** 677
[4] Johnston R L 2002 *Atomic and Molecular Clusters*, Taylor and Francis, London
[5] Jensen P 1999 *Rev. Mod. Phys.* **71** 1695
[6] Bardotti L, Jensen P, Hoareau A, Treilleux M, Cabaud B, Perez A, Cadete A and Aires A 1996 *Surf. Sci.* **367** 276
[7] Papathanakos V and Evangelakis G A 2002 *Surf. Sci.* **499** 229
[8] Sun D Y and Gong X G 2000 *Surf. Sci.* **445** 41
[9] Deltour P, Barrat P and Jensen P 1997 *Phys. Rev. Lett.* **78** 4597
[10] Haberland H and Moseler M 1995 *Phys. Rev. B* **51** 11061
[11] Bardotti I, Prével B, Mélinon P, Perez A, Hou Q and Hou M 2000 *Phys. Rev. B* **62** 2835
[12] Hou Q, Hou M, Bardotti L, Prével B, Mélinon P and Perez A 2000 *Phys. Rev. B* **62** 2825
[13] Kong J, Franklin N R, Zhou C, Chapline M G, Peng S, Cho K and Dai H 2000 *Science* **287** 622
[14] Dilon A C and Heben M J 2001 *Appl. Phys. A: Mater. Sci. Process* **72** 133
[15] Wang Q Y, Challa S R, Sholl D S and Johnson J K 1999 *Phys. Rev. Lett.* **82** 956
[16] Cvitas M T and Siber A 2003 *Phys. Rev. B* **67** 193401
[17] Wei S and Johnson J K 2003 *Phys. Rev. Lett.* **91** 15504
[18] Calbi M M, Gatica S M, Bojan M J and Cole W M 2001 *J. Chem. Phys* **115** 9975
[19] Zhang Y and Dai H 2000 *App. Phys. Lett.* **77** 3015
[20] Bagci V M K, Gulseren O, Yildirimi T, Gedik Z and Ciraci S 2002 *Phys. Rev. B* **66** 45409
[21] Dendzik Z, Kośmider M, Skrzypek M and Gburski Z 2004 *J. Mol. Struct.* **704** 203
[22] Aziz R A 1993 *J. Chem. Phys.* **99** 4518
[23] Stan G, Bojan M J, Curtarolo S, Gatica S M and Cole M 2000 *Phys. Rev. B* **62** 2173
[24] Guo Y and Karasawa N 1991 *Nature* **351** 464
[25] Walther J H, Jaffe R, Halicioglu T and Koumoutsakos P 2001 *J. Phys. Chem. B* **105** 9980